Iran. J. Biotechnol. April 2023;21(2): e3344 DOI: 10.30498/ijb.2023.337246.3344

Research Article

Molecular Dynamics Simulation of Antimicrobial Peptide CM15 in *Staphylococcus Aureus* and *Escherichia coli* Model Bilayer Lipid

Davood Zaeifi, Ali Najafi, Reza Mirnejad*

Molecular Biology Research Center, Systems Biology and Poisonings Institute, Baqiyatallah University of Medical Sciences, Tehran, Iran.

**Corresponding author*: Reza Mirnejad, Molecular Biology Research Center, Systems Biology and Poisonings Institute, Baqiyatallah University of Medical Sciences, Tehran, Iran. Tel: +98-2182482554, Fax: +98-2187555253, E-mail: rmirnejad@bmsu.ac.ir

Received: 2022/04 /12; **Accepted:** 2022/10/24

Background: In animals and plants, antimicrobial peptides (AMPs) are crucial components of defense mechanisms, as they play a crucial role in innate immunity, which protects hosts from pathogenic bacteria. The CM15 has attracted considerable interest as a novel antibiotic against gram-negative and positive pathogens.

Objective: The aim of this study was to investigate the permeation potential of the CM15 with membrane bilayers of *Staphylococcus aureus* and *Escherichia coli*.

Material and Methods: The bilayer membranes of *Escherichia coli* and *Staphylococcus aureus* were modelled with the resemblance in lipid composition to its biological sample. This study followed Protein-Membrane Interaction (PMI) through successive applications of molecular dynamics simulation by GROMACS and CHARMM36 force field for two sets of 120-ns simulations.

Results: Significant results were obtained from analyzing the trajectory of the unsuccessful insertion of CM15 during simulation. Our data suggested that Lysine residues in CM15 and Cardiolipins in membrane leaflets play a crucial role in stability and interaction terms.

Conclusion: The obtained results strengthen the insertion possibility through the toroidal model, which should consider for further studies on AMPs interaction.

Keywords. Antimicrobial peptide, Cardiolipin, CM15, Molecular dynamic, TOCL

1. Background

Contemporary medicine mostly depends on antibiotics to deal with bacterial infections. However, the growing resistance in bacteria against antibiotics turned into a significant threat to health and food security in the world, which requires constant research for finding new synthetic and natural antibacterial agents and antimicrobial peptides (AMPs) among the candidates. The AMPs usually have a wide range of activities against fungi and pathogenic bacteria. Several intrinsic eukaryotic peptides can influence bacterial membranes and other targets (1). This is in contrast with antibiotics that usually target specific proteins like the bacterial ribosome.

AMPs in higher eukaryote organisms are known as 'host defense peptides' due to their additional immunomodulatory activities in modulating immune and inflammatory responses to infections. Moreover, they were found to be more effective and are a slower resistance generation in compare with typical antibiotics (2, 3).

With significant differences in the type of membrane lipid composition in various bacteria membranes, the antibiotics expand the ability to induce lateral phase segregation. Due to this, the bilayer with anionic and

zwitterionic lipids are at a higher risk of being affected by antibiotics than those with mainly anionic lipids (4, 5). Most literature suggested mix lipids consisting of Palmitoyloleoyl phosphatidylethanolamine (POPE or PE) and Palmitoyloleoyl phosphatidylglycerol (POPG or PG) are significant and ideal components for the bacterial membranes study model due to lower transition temperature and stability versus Palmitoyloleoyl phosphatidylcholine (POPC or PC) lipid bilayer. Moreover, PE plays a crucial role in folding and membrane protein permeation. (6-8).

In comparison with PC, PG has two more acceptor units and a negative net charge at physiological pH, plus the capability of PE to form a hydrogen bond, making the PG:PE mixed-bilayer a suitable candidate for the bactericidal membrane study. The presence of the phosphatidylethanolamine headgroup helps accurate placement and analysis of protein folding and membrane permeabilization (6, 7, 9). The PG and Cardiolipin (TOCL1 or CL) lipids are predominant anionic components that allocate at least 15% of the bacterial membrane bilayer. It consists of PG or CL or both, without assuming that it is a gram-positive or negative microorganism. Joining these components with lipopolysaccharides and lipoteichoic acid provides the selectivity of cationic AMPs against bacteria (10, 11).

AMPs produced single-channel conductances on the surface of lipid bilayers, and both enantiomers (D and L) caused equivalent amounts of electrical conductivity. The all-D enantiomer of CM15 keeps its competitive biological acting like resistancy to enzymatic degradation against a wild range of bacteria (12). The cationic linear AMPs interact with negatively charged cell wall components, known to permeabilize membranes non-stereospecificity (equal MIC for L- and D-form), so the interaction of CM15 with bacterial cell wall components is non-stereospecific (13). Notably, the reverse ("retro") and all-D reverse ("retroenantio") sequences respond to specific bacterial strains (such as *B. subtilis*, *E. coli*, and *S. pyogenes*) and are not active against *S. aureus* or *P. aeruginosa*. Therefore, it seems that chirality does not affect the efficacy of peptides, while in some cases, it is necessary to take sequence order and direction of amide bonds into account (14)

2. Objective

A potential solution to the issue of antibiotic resistance is antimicrobial peptides (AMPs); however, having an efficient design of APMs that are both active and not toxic needs to realize the action mechanism. Therefore, this study explored the interaction and permeation possibility of the CM15 with *Staphylococcus aureus* (gram-positive) and *Escherichia coli* (gram-negative) membrane bilayer by successive application of molecular dynamics simulation.

3. Material and Method

3.1. Lipid Bilayer Preparation

Lipid bilayer generated by CHARMM membrane builder server (15). *S. aureus* and *E. coli* consisted of a mixture of PG, PE, and CL lipid types. Each membrane consisted of 78 lipid molecules and water molecules, as shown in **Table 1,** which was minimized for 1000 steps and equilibrated with fixed pressure and temperature conditions in the server six times for 500 PS in each step (11). In addition, a 5-ns simulation was conducted under NPT conditions to equilibrate the system. The area per lipid was calculated by Grid MAT-MD v2.0 in X/Y and independent Z direction in both systems (16).

3.2. Peptide-Lipid Systems Preparation

The progress began with a one ns simulation of CM15 (PDB code: 2JMY with KWKLFKKIGAVLKVL sequence) as the best model in water to achieve proper conformation (17). The systems consisted of 5330 total

Table 1. The systems composition.

	Lipid Type			TIP3	Na	Cl	Surface area (nm^2)
	PG	PE	CL				
E. coli	12	62	4	5330	25	15	25.273
S. aureus	46	0	32	8786	96	24	35.938

water molecules and were neutralized by distributing Na^+ ions together with Cl^- ions at a final concentration of 0.1 M of NaCl for both *E. coli* and *S. aureus* systems (**Table 1**). CM15 was positioned at 30 Å from bilayer head groups (**Supplementary 1**).

3.3. Molecular Dynamic Simulation Protocol

Overall, for each peptide-lipid system, 120 ns simulations were carried out. Both simulations were done under fixed pressure and temperature; however, normal dimension fluctuation along the membrane was permitted (NP_zT). Periodic boundary conditions were set for all directions so that CM15 could freely diffuse in water. Conservative restraining potential was applied where the center of mass (C.O.M) of CM15 left the buffer zone. No external force was exerted at the buffer zone against CM15 before attaining the boundary. The average area per lipid leaflet was ~49.5 $Å^2$ and ~ 58.7 $Å^2$ for *E. coli* and *S. aureus* respectively, after energy minimization. However, at the simulation's starting point, in both cases, there was a decrease of about ~5%. The temperature was set to 303.15 K by the Langevin dynamics system. Nose-Hoover temperature coupling method was used to maintain the temperature while the pressure remained constant at 1 bar using the semi-isotropic Parrinello-Rahman method with tau-p of 2 PS to achieve accurate results (18).

The latest update of the CHARMM36 force field was employed to build the mentioned systems. Both simulations were carried out under GROMACS (version 2016.3) with a 2 fs time-step and all covalent and hydrogens bonds were limited with the help of the LINCS algorithm. The electrostatic and vdW energy short-range cut-off was set to 12 Å with a switching distance of 10 Å. With periodic boundary conditions, the Particle Mesh Ewald (PME) method in cubic interpolation with a grid spacing of 1.6 Å for Fast Fourier Transform (FFT), was used for the calculation of long-range electrostatic interaction.

3.4. Data Analysis

All analyses were performed using GROMACS, VMD (19), and MATLAB (20). Visualizing structures was carried out using Chimera (21). The distance calculation was performed along with considering the lipid phosphorus atom and C.O.M of the peptide. The analysis of membrane thickness and fluctuations was performed using g_lomepro (17) and mapped in MATLAB. The electrostatic and vdW interaction energy was analyzed using g_mmpsa (22). The effective hydrogen bond between CM15 atoms at a 3 Å distance of bilayer membrane was taken into account. In addition, the secondary structures and peptides' C.O.M (for in-contact residues) during the simulation was calculated using DSSP (23) and GROMACS, respectively.

4. Results

Interactions of CM15 with both model membrane was evaluated, and the findings showed that peptide conformation changed. In addition, its behavior during the simulation was monitored. The layer in contact with the peptide was considered the upper layer.

4.1. Interaction of CM15 and Bilayer Lipids

The overall conformation change of interactions in CM15 at 120 ns interval is demonstrated in **Figure 1** for *S. aureus. E. coli* interactions from the first contact to completion were prepared and presented. The peptide could not pass the phosphorus borderline. The CM15 can diffuse throughout the simulations without limitation in water and can choose any orientation it first reaches the bilayer. Therefore, unbiased analysis of the initial peptide-lipid contact is achievable.

4.2. Center of the Mass (C.O.M)

Detecting structures using optical techniques is not free of a hindrance when they are used for peptide-membrane systems. The details and dynamic processes between peptides and membranes cannot be measured directly. It is assumed that the CM15 penetrates the lipid if its C.O.M passes the membrane phosphorus atoms. Trajectories from 120 ns simulations of both interactions in **Figure 2B** and **2C** demonstrate that the CM15 binds to both lipids and causes significant membrane fluctuations. In both CM15 simulations, the peptide can choose an orientation close to parallel to the membrane normal (**Fig. 2A**). Still, this peptide only resides in the upper leaflet instead of spanning the whole bilayer. There was also no pore formation while the slight perturbation barely affected the bilayer.

As described earlier, CM15 is freely diffused in water from 30 Å away to reach the bilayer in an appropriate orientation during simulation. The analysis showed CM15 contact from N-terminus in both systems.

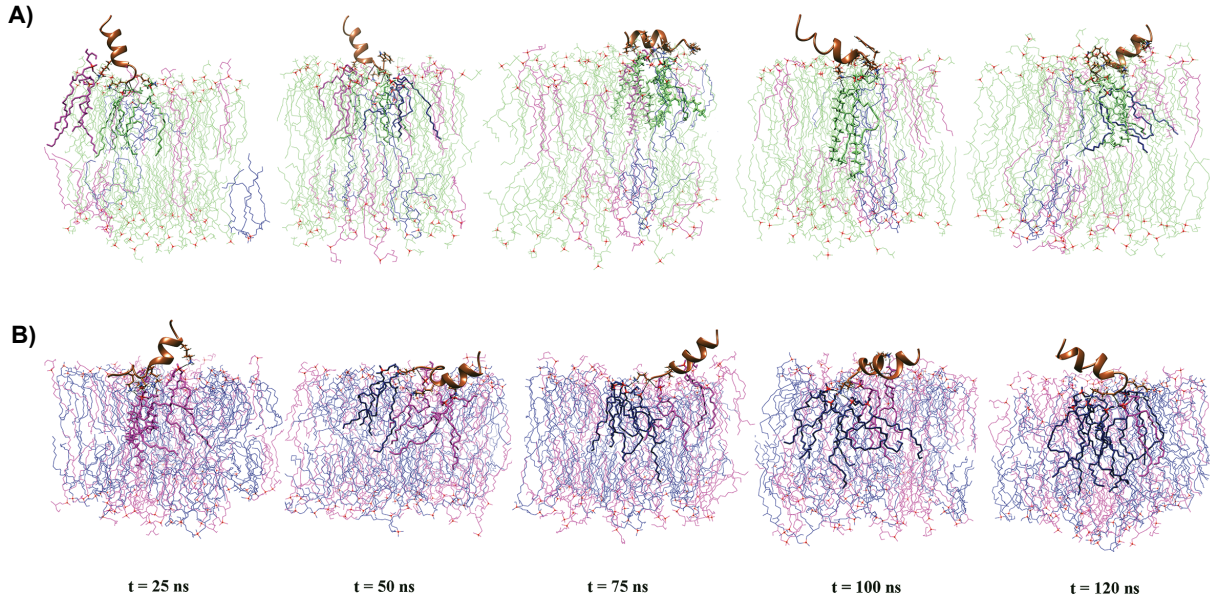

Figure 1. Representative structures of CM15. A) in *E. coli* and **B)** in *S. aureus* systems. The lateral views of structural changes throughout the simulations at 120 ns intervals. Each peptide structure, except for the initial structures, are shown at 120 ns interval is the center of clustering 120 ns conformations. Phosphorus and peptides of lipid are highlighted with red and brown respectively.

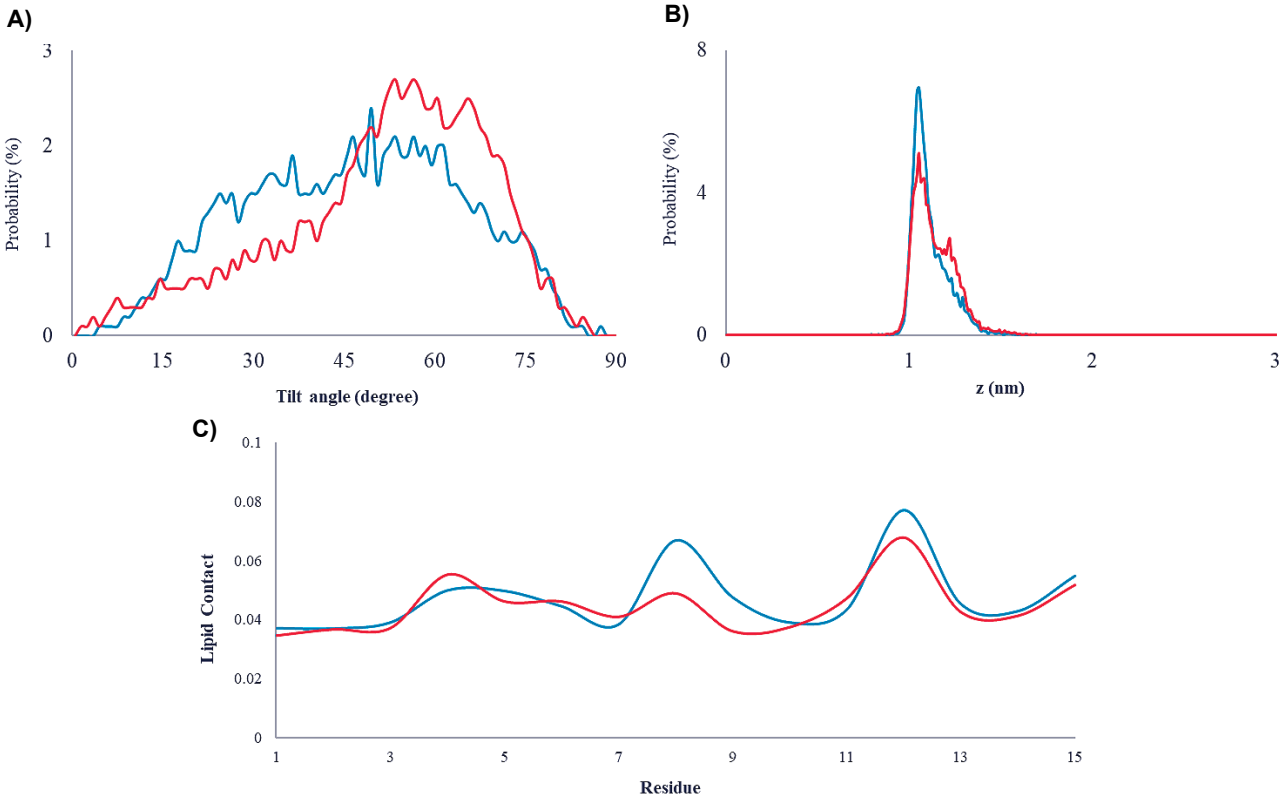

Figure 2. Histograms of CM15. A) tilt angles, **B)** C.O.M., and **C)** peptide atoms count in contact with lipid molecule in simulations *S. aureus* (orange) and *E. coli* (blue). The peptide tilt angle is the angle formed by the z-axis and a line connecting the Cα atoms of residue 5 and 12 of CM15. The lipid contact is determined as the non-hydrogen atoms count within 3Å of membranes. The findings are represented by the total number of atoms in a residue. The resolution of histograms of tilt angles and C.O.M. is 1 degree and 0.1 nm, respectively.

Three residues (LYS-1, LYS 6, and VAL-14) had a stronger connection to the membrane compared to other residues; LYS-6 was the most in contact residue in both systems, and VAL-14 was so in the *S. aureus* system. Root mean square deviation indicated a small shift in backbone conformation of the hollo system at 75 ns from 0.29 nm to 0.41 nm during the 120 ns simulation (**Fig. 3A**). In addition, in the *S. aureus* system, the peptide showed more flexibility due to higher RMSD values, as confirmed by RMSF results (**Fig. 3B**).

4.3. Solvent Accessibility in CM15

The residue solvent exposure is determined based on the relatively accessible surface area or relative solvent accessibility (RASA or RSA) of a protein residue. It can be calculated by the formula (24):

RSA=ASA/MaxAsA

So ASA is the solvent-accessible surface area, and MaxASA represents the maximum possible solvent-accessible surface area for the residue. The ASA and

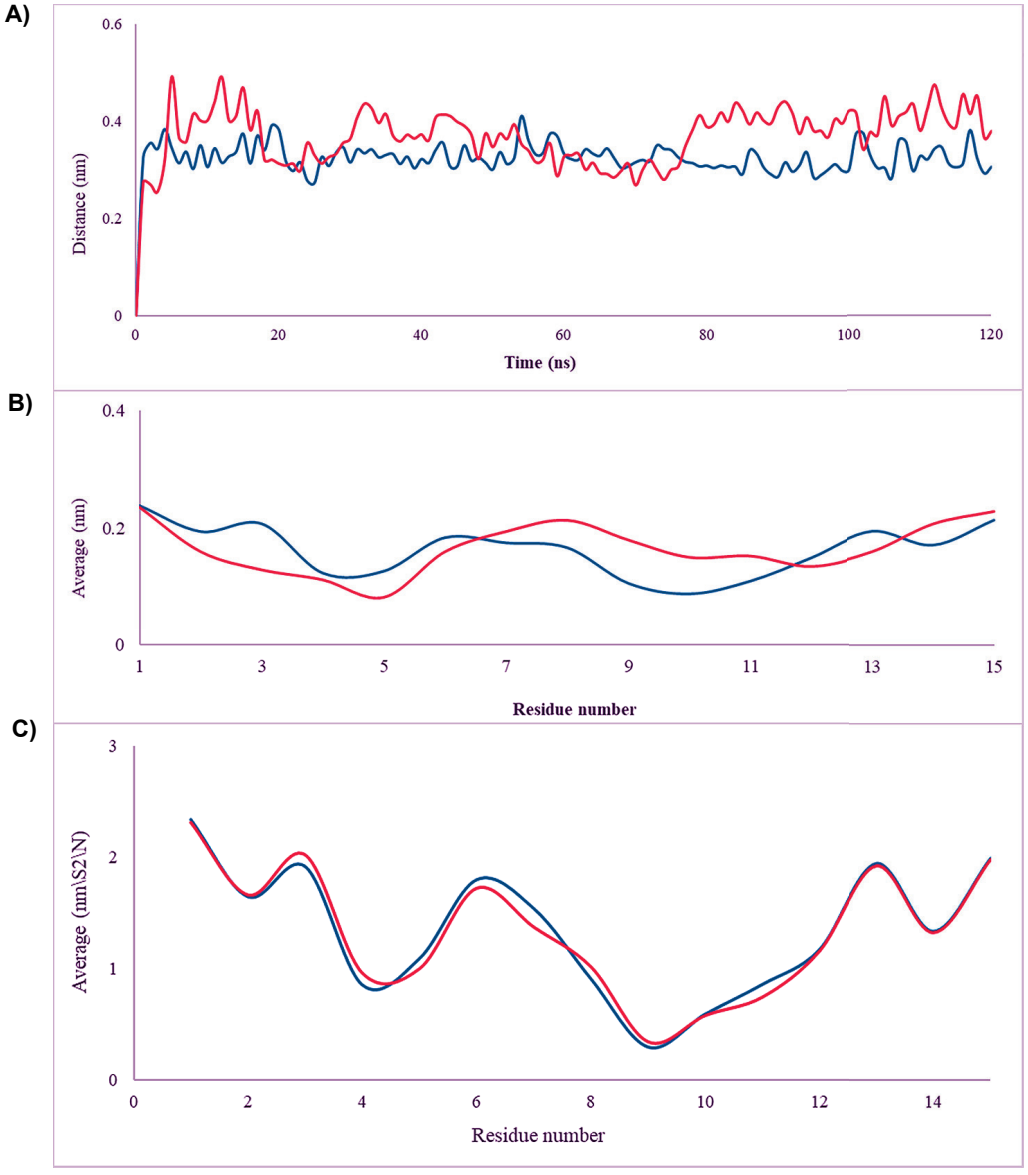

Figure 3. CM15 backbone. A) RMSD and **B)** RMSF analysis of all-atom MD trajectories for *S. aureus* (orange) and *E. coli* (blue) systems during the 120 ns simulation. **C)** The accessibility of residues duri ng the molecular dynamic process of CM15 evaluated Relative Accessible Surface Area (RASA) of each residue in *S. aureus* (orange) and *E. coli* (blue) systems.

MaxASA are commonly measured in Å.

The MaxASA values determined by Gly-X-Gly tri-peptides are used to determine the relative solvent accessibility of the residue side-chain. Where X represents the residue of interest. Several MaxASA scales are available (25).

The accessibility of CM15 residues was examined by determining the Relative Accessible Surface Area (RSA) of each residue during the molecular dynamic simulation (**Fig. 3C**).

4.4. Energy Landscape

Every macromolecule demonstrates functional motions that are based on the complex correlation in the atomic motions. These internal motions are required to achieve efficient functioning, such as conformation modification to different biological environments and etcetera. Several internal motions in protein molecules make it hard to interpret. Principal component analysis can be used to decrease many dimensions of the data set down to the major principal components that only demonstrate changes that display the global motion of the protein with the key information. According to the first stable contact in both membranes by LYS -1, LYS-3, and LYS-6 in systems, CM15 binds to the *E. coli* membrane faster as was expected due to electrostatic interaction of cationic peptide and an anionic net charge of bilayer membranes. In addition, the vdW, and electrostatic interaction energy in both systems, which is demonstrated in **Figures 4C** and **4D,** reveal approximately three-fold at z ≥10 Å for electrostatic interaction energy.

The free energy landscape (FEL) and internal motion of the system analysis give us a better image of the conformational space of protein in terms of energy and time. The results of EFL only depend on the risk of occurrence of a mixture of certain data points, which are converted into a free-energy value using a straightforward relationship. As illustrated in **Figures 4A** and **4B**, the free energy landscapes are projected on the first two key elements of the CM15 and *E. coli* and *S. aureus* membrane complexes interaction. The form and size of the minimal energy area (marked as red) in the free energy contour map means that the stability of the complex is higher. The centralized and small blue spots indicate that the pertinent complex has higher stability. The conformational variability of the peptide was obtained by the analogy of the radius of gyration and RMSD to the average structure. **Figures 4A** and **4B** represent a mapping of all possible Free Binding Energy in the time scale. According to free energy landscapes, the stability of a protein is illustrated in terms of Gibbs free energy. Here, the EFL and internal motion of the two systems were analyzed through FEL for 120ns simulations and plotted as 3D graphs. According to FEL calculation, the two systems only had one energy minima in the 120 ns simulation. The model for the *S. aureus* had higher stability with some intermediate states compared to *E. coli*. In addition, the distribution of peptide backbone RMSD demonstrated a normal distribution and a decline in conformational flexibility.

4.5. Folding of CM15 During the Simulation

Because of the importance of secondary structure in the many proposed mechanisms of antimicrobial peptide action, the results of computational simulations are often examined for data related to secondary structure formation. Various computational studies with 120 ns timeframes report secondary structure formation when using individual peptides biased toward the membrane and/or various constrained membranes (26). It is theorized that peptides with different aspects, like secondary structure, chain length, net charge, etcetera, exhibit different biological processes. Peptide folding takes a lot of time; in this respect, most of the antimicrobial peptide studies here rely on folding, α-helical conformation, and the starting structure of the peptide. However, extended conformations for the peptides are used because MD simulations are intended to be utilized as a pre-experimental screening method for computationally designed novel peptides of which secondary structures are not a priori known. Recent research has suggested the specificity of the interacting site to the bacterial membrane (27). The CM15, like many other AMPs, forms the α-helical conformation in contact with lipids. The distribution of the most frequent conformations of the CM15 was obtained using DSSP. In the analysis, CM15 is found to form α-helical structures equal to random coils and turns (**Supplementary 2**).

Our results revealed the tendency of CM15 to form an α-helix and Π-helix in *S. aureus* and turn in *E. coli* during contact with lipid, which suggests CM15 tendency to form a linear shape. **Table 2** shows the conformational element of this distribution for the appearance of secondary structure.

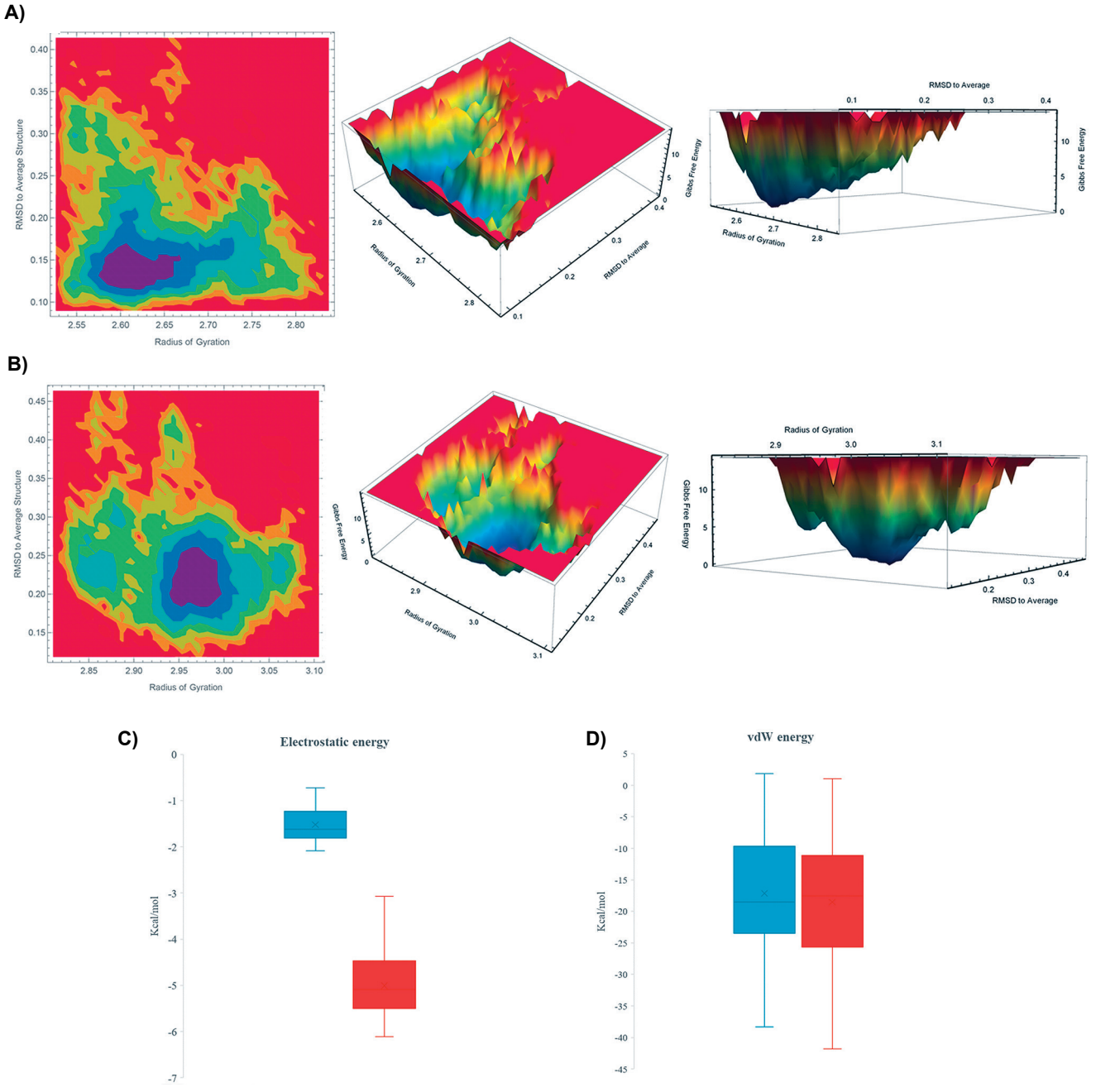

Figure 4. The 2D and 3D free energy landscape and internal motion of CM15 interactions with **A)** *E. coli* and **B)** *S. aureus* membrane. The valleys which are in purple reveal the minimal free binding energy during the simulation. The average conversion of **C)** electrostatic and **D)** van-der-Waals interaction energy in CM15: *S. aureus* (orange) and *E. coli* (blue).

4.6. Lipid Area and Thickness Fluctuation in Membranes Upper Leaflet

A key role is played by charged amino acids in the control of the actions of integral and peripheral membrane proteins and the cells that disrupts peptides. Atomistic molecular dynamics literature has uncovered mechanisms of membrane binding and translocation of charged protein groups. However, the effect of the full diversity of membrane physicochemical properties and topologies is not studied thoroughly (28). Biological membranes function as a host of protein with critical functions and as protective shells that block uncatalyzed permeation of

Table 2. The highest number of salt-bridge and a hydrogen bond between CM15 and bilayers for each element.

System	H-bound	Salt-bridge	In contact res
S. aureus	7.5%	27%	POPG
	1.5%	26.2%	TOCL1
E. coli	1.2%	17.9%	POPG
	6.2%	53.3%	POPE
	6.62%	0.02%	TOCL1

polar and charged molecules effectively. This perception has ruled for many years, and it is comprehended in terms of the energetics of ion translocation across an oily slab of the membrane. Still, studies have recently shown that cell membranes are not impenetrable. Taking into account that arginine (Arg) and lysine (Lys) as basic amino acids play an important role in the function, structure, and actions of protein of different cell-perturbing, there is a need to examine the interactions of charged protein groups with biological membranes at the molecular level (28). During the simulation, the changes in area per lipid (upper leaflet) were calculated based on the fluctuation of the headgroup phosphorus atom, which was stable in both systems. (**Fig. 5A**).

By lipid bilayer thickness calculation, this study showed that the models demonstrated identical curves for the probable initial insertion of a lipid headgroup into the hydrophobic core of the lipid bilayer, in which the formation of single-sided water defects may accompany. This can be a promising start considering the importance of trivial defects in membranes to stimulate transmembrane peptides, proteins, drugs, and many other polar solutes. It is not easy to explain the energetic reason for similarity; however, we can highlight a basic underlying physical basis of the process (**Fig. 5B**) (29).

Based on the changes in the number density profiles and permeability of water, we can predict the presence of a perturbed bilayer structure (**Fig. 5C**). Given these profiles, structural changes are the biggest for PG: TOCL.

Since CM15 peptide could not penetrate both modeled lipids, the phosphorus transition was calculated through the XYZ axis by g_lomepro and mapped with MATLAB in **Supplementary 3**, demonstrating the tension and fluctuations in the upper leaflet of lipids during the simulation.

5. Discussion

Dynamic increase of resistance in bacterial infectious diseases constantly needs the development of new elements against them. The understanding at the molecular level of the mechanisms and interactions of natural host-defense peptides or AMPs is a major step in argumentative design and developing compounds based on their function (30).

As mentioned above, the conservative restraining potential was applied where the center of mass of CM15 extended beyond the buffer zone; and no external force was exerted at the buffer zone against CM15 before attaining the boundary. After energy minimization, the average area per lipid leaflet was ~49.5 $Å^2$ and ~ 58.7 $Å^2$ for *E. coli* and *S. aureus,* respectively. The CM15 can diffuse freely during the simulation and take any orientation when it hits the bilayer for the first time. Therefore, we can have an unbiased analysis of the initial peptide-lipid contact. As shown, the whole combination changes of interactions in CM15 at 120 ns interval for *S. aureus* and *E. coli* interaction indicated that the peptide could not pass the phosphorus borderline. The lateral view of CM15 interaction in *E. coli* and *S. aureus* systems indicates structural variations throughout the simulations at 120 ns intervals. Each peptide structure at 120 ns interval, except for the initial structures, constitutes the center of clustering 120ns conformation. Yi Wang et al. found that CM15 simulations in POPG:POPC and POPC meant that the peptides were inserted into both lipid bilayers (26).

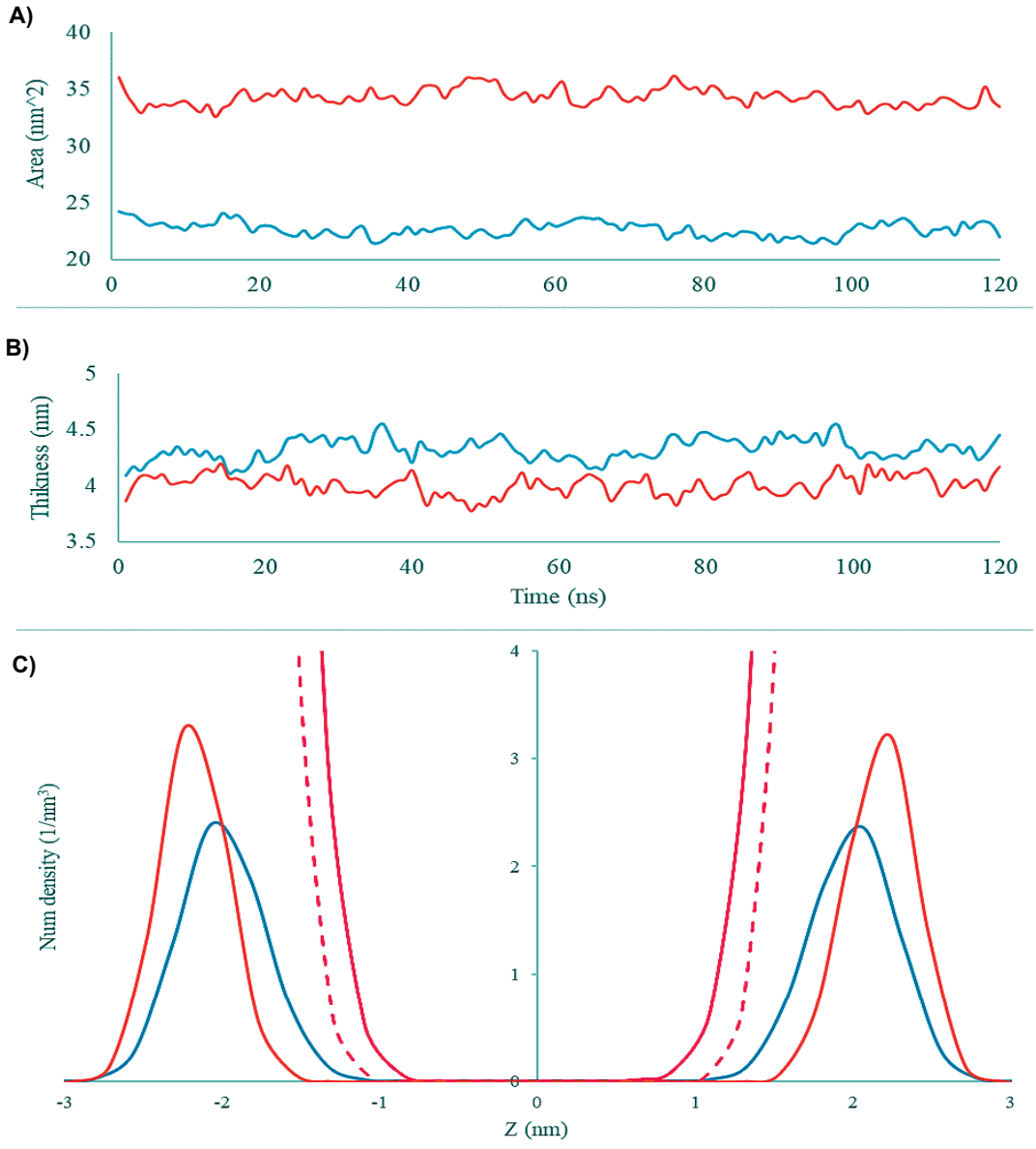

Figure 5. Lipid Area and Thickness Fluctuation in the Membranes Upper Leaflet. A) The lipid area fluctuations in *S. aureus* (orange) and *E. coli* (blue) system in X/Y and independent Z direction during the simulation. **B)** The thickness fluctuations in *S. aureus* (orange) and *E. coli* (blue) system in the Z direction to the membrane center of mass during the simulation. **C)** Changes in bilayer structure and water permeability upon the interaction with CM15. Number density profiles of phosphorus atoms (*S. aureus* (orange) and *E. coli* (blue)) and water oxygen atoms (*S. aureus* (dashed curve) and *E. coli* (red)) in systems.

This finding is not expectable to some extent because of the non-hemolytic nature of CM15 (31). As the simulation results indicated, it is not possible to conclude that CM15 can achieve the selectivity for bacterial membranes only by causing pore formation in POPG: POPC.

AMPs are designed to protect humans against microbial infections; still, the mechanism and penetration process is not transparent (32). Generally, most gram-negative species contain a significant amount of anionic and zwitterionic components in their lipids, so the mechanism of inducing lateral phase separation is more effective for gram-positive species (11). Performed thermodynamic analysis in the current study did not present any

record for lateral separation in membrane mixture of PC:CL, except for PE:CL; which is the most important mechanism of inducing (33).

Many studies noted the dominancy of PE over PC due to the higher hydrocarbon chain, higher temperature phase transition, smaller cross-sectional area, and stronger inter-lipid contacts at the microbial inner membrane (34-37). Recent studies on the cationic AMPs on POPC bilayer alone or in mixed form revealed that the CM15 could penetrate inside, while our results showed ambiguities (26). First, as the analysis of Domenech *et al*. suggested, significant lateral phase separation could not be observed in the presence of Cardiolipin in POPC alone or in mixed, which confirms our results (33). On the other hand, POPC bilayers alone or in the mixed form are considered biological membranes for some fungus (like *C. albicans* and *Erythrocyte*) and animals, which does not make it a proper model for microbial study (38, 39). Furthermore, in the case of penetration, the suggested AMPs lose their advantage by being converted into a miss-functional protein in the host cell (40).

During the observation and analysis of this study, it was found that the perturbed bilayer structure was also evident from variations of bilayer structure and permeability of water upon the interaction with CM15. The profiles of the density of phosphorus atoms *S. aureus*, *E. coli*, water oxygen atoms *S. aureus*, and *E. coli* in systems illustrated in **Figure 5C** indicate that these structural and profile changes seem to be the biggest for PG: TOCL. Many articles have suggested that aggregation and pore formation in outer membrane bacterial cells treated by AMP leads to membrane permeabilization (3, 18, 41). Analysis of trajectory on membrane fluctuation in **Figure 5C** revealed that the CM15 tried to form a pore with tensioning on the bilayer. According to this, the hypothesis of pore formation with the toroidal model was strengthened (42). Several peptides attach to a lipid monolayer and form a pore through aggregation, increasing inner pressure and decreasing the surface tension and penetrating inside (43). Given this hypothesis, α-helix structural stability due to toroidal model inducing plays a crucial role in targeting membrane, which confirms our results (32).

In our study, CM15 within the simulation is freely diffused in water from 30 Å away to reach the bilayer in a suitable direction. The analysis showed that CM15 attaches to the membrane in both systems through the N-terminus. Three residues (LYS-1, LYS 6, and VAL-14) had stronger connections than others, and LYS-6 was the most in contact residue in both systems; and VAL-14 was so in the *S. aureus* system. Root mean square deviation calculation showed a slight change in backbone conformation in the holo system at 75 ns from 0.29 nm to 0.41 nm during the 120 ns simulation. The peptide showed more flexibility in the *S. aureus* system due to higher RMSD values.

Due to cationic residues and zwitterionic components of the membrane, including Cardiolipins, the first contact residue in both systems was formed by the N-terminus of AMP, which improved the possibility of contact or even permeability. The distribution of in-contact residues with membrane lipids demonstrated the significant impact of Cardiolipin on the possible permeability of the lipids due to the distribution of Cardiolipin in the interaction surface with CM15 (44, 45). The importance of Cardiolipin in prokaryotic cell function, specifically the regulation of cell function at a higher level in the organization of energy transducing, was investigated, which revealed the contacts stabilizer role of Cardiolipin between proteins through the VdW contacts and the phosphate groups for interaction with hydrogen bonds (46). The electrostatic potential energy in **Figure 4C** and conformational elements (**Table 2**) indicated the presence of a more substantial positive charge for CM15 interaction with *E. coli* versus *S. aureus*. In addition, as the Π-helical region in the peptide is significantly energetic, the peptide can take proper orientation along with stabilizing the native state of the protein without disrupting the structure, which depends on the specificity of interaction (47). Our data in the *S. aureus* system revealed this tendency for forming Π-helix, which forms a more compact structure. The stability of CM15: *E. coli* and *S. aureus* complexes was examined using free energy landscape binding energy calculations, molecular dynamics simulation, molecular docking, and free energy decomposition. According to docking results, the binding of CM15 with gram-negative family bacteria had more vital binding energy compared to *S. aureus.*

In summary, in the case of any probable penetration later, obtained results consider the CM15 more suitable for gram-negative family bacteria. However, a longer time scale, more extensive contact area, and simultaneous use of multiple AMP molecules, through forming a pore could provide more precise details on AMPs' interaction

with the bacterial membrane. Still, the *in vivo* function of the peptides is complicated, which can be due to the enormous diversity of interactions with small-molecule agents. Two sets of 120 ns simulations were performed, and a significant result was obtained for the unsuccessful insertion of CM15 during the simulation. Our data express that Lysine residues in CM15 and Cardiolipins in membrane leaflets play a crucial role in stability and interaction terms. The obtained hints from these results prestress the insertion possibility in a toroidal model, which should be considered for further studies on AMPs interaction.

6. Conclusion

As a result of preparing data from fluctuations, and considering the phosphorus atoms as borderline, transmission of CM15 through the upper leaflet of the membrane became inefficient. The LYS residues in CM15 and Cardiolipin in the membrane bilayer enhanced the stabilization and modality interaction of the peptide.

Given the results, it is possible to modify the AMP function using small-molecule secondary structure regulators. This can be seen as an opportunity for the future development of AMP-based antimicrobial agents. With a more profound perception of the molecular events that cause membrane disruption, improvement of peptide design can be facilitated, and it is possible to develop new antibiotics using mechanistic principles and AMP structure.

Our study suggested a deeper understanding of the performance process of AMPs and indicated that gram-negative bacteria are more appropriate for this hypothesis. The use of other Gram-negative bacteria such as *Enterobacter*, including *E. aerogenes* or *E. sakazakii*, is also recommended. Peptides other than CM15 can also be used to confirm this. Expanding the understanding of AMPs paves the way for the dealing of many bacteria.

Conflicts of Interest:

The authors declare any conflicts of interest.

References

1. Kesidis A, Depping P, Lode A, Vaitsopoulou A, Bill RM, Goddard AD, *et al*. Expression of eukaryotic membrane proteins in eukaryotic and prokaryotic hosts. *Methods*. 2020;**180**:3-18. doi: 10.1016/j.ymeth.2020.06.006.
2. Moghaddam MM, Abolhassani F, Babavalian H, Mirnejad R, Azizi Barjini K, Amani J. Comparison of *in vitro* antibacterial activities of two cationic peptides CM15 and CM11 against five pathogenic bacteria: Pseudomonas aeruginosa, Staphylococcus aureus, Vibrio cholerae, Acinetobacter baumannii, and Escherichia coli. *Probiotics Antimicrob Proteins*. 2012;**4**(2):133-139. doi: 10.1007/s12602-012-9098-7.
3. Moravej H, Moravej Z, Yazdanparast M, Heiat M, Mirhosseini A, Moosazadeh Moghaddam M, *et al*. Antimicrobial Peptides: Features, Action, and Their Resistance Mechanisms in Bacteria. *Microb. Drug Resist (Larchmont, NY)*. 2018;**24**(6):747-767. doi: 10.1089/mdr.2017.0392.
4. Ratledge C, Wilkinson S. An overview of microbial lipids. *Microbial lipids*. 1988;**1**:3-22.
5. Ratledge C, Wilkinson S. Fatty acids, related and derived lipids. *Microbial lipids*. 1988;**1**:23-52.
6. Bogdanov M, Dowhan W. Phosphatidylethanolamine is required for *in vivo* function of the membrane-associated lactose permease of Escherichia coli. *J Biol Chem*. 1995;**270**(2):732-739. doi: 10.1074/jbc.270.2.732.
7. Bogdanov M, Dowhan W. Phospholipid-assisted protein folding: phosphatidylethanolamine is required at a late step of the conformational maturation of the polytopic membrane protein lactose permease. *EMBO J*. 1998;**17**(18):5255-5264. doi: 10.1093/emboj/17.18.5255.
8. Domenech O, Torrent-Burgues J, Merino S, Sanz F, Montero MT, Hernandez-Borrell J. Surface thermodynamics study of monolayers formed with heteroacid phospholipids of biological interest. *Colloids Surf B Biointerfaces*. 2005;**41**(4):233-238. doi: 10.1016/j.colsurfb.2004.12.012.
9. Dickey A, Faller R. Examining the contributions of lipid shape and headgroup charge on bilayer behavior. *Biophys J*. 2008;**95**(6):2636-2646. doi: 10.1529/biophysj.107.128074.
10. Epand RM, Epand RF. Lipid domains in bacterial membranes and the action of antimicrobial agents. *Biochim Biophys Acta*. 2009;**1788**(1):289-294. doi: 10.1016/j.bbamem.2008.08.023.
11. Epand RM, Rotem S, Mor A, Berno B, Epand RF. Bacterial membranes as predictors of antimicrobial potency. *J Am Chem Soc*. 2008;**130**(43):14346-14352. doi: 10.1021/ja8062327.
12. Wade D, Boman A, Wahlin B, Drain CM, Andreu D, Boman HG, *et al*. All-D amino acid-containing channel-forming antibiotic peptides. *Proc Natl Acad Sci U S A*. 1990;**87**(12):4761-4765. doi: 10.1073/pnas.87.12.4761.
13. Bucki R, Janmey PA. Interaction of the gelsolin-derived antibacterial PBP 10 peptide with lipid bilayers and cell membranes. *Antimicrob Agents Chemother*. 2006;**50**(9):2932-2940. doi: 10.1128/AAC.00134-06.
14. Sato H, Feix JB. Peptide-membrane interactions and mechanisms of membrane destruction by amphipathic alpha-helical antimicrobial peptides. *Biochim Biophys Acta*. 2006; **1758**(9):1245-1256. doi: 10.1016/j.bbamem.2006.02.021.
15. Wu EL, Cheng X, Jo S, Rui H, Song KC, Davila-Contreras EM, *et al*. CHARMM-GUI Membrane Builder toward realistic biological membrane simulations. *J Comput Chem*. 2014; **35**(27):1997-2004. doi: 10.1002/jcc.23702.
16. Allen WJ, Lemkul JA, Bevan DR. GridMAT-MD: A grid-based membrane analysis tool for use with molecular dynamics. *J Comput Chem*. 2009;**30**(12):1952-1958. doi: 10.1002/jcc.21172.
17. Respondek M, Madl T, Gobl C, Golser R, Zangger K. Mapping the orientation of helices in micelle-bound peptides by paramagnetic relaxation waves. *J Am Chem Soc*. 2007;**129** (16):5228-5234. doi: 10.1021/ja069004f.
18. Fantner GE, Barbero RJ, Gray DS, Belcher AM. Kinetics

of antimicrobial peptide activity measured on individual bacterial cells using high-speed atomic force microscopy. *Nat Nanotechnol*. 2010;**5**(4):280-285. doi: 10.1038/nnano.2010.29.
19. Humphrey W, Dalke A, Schulten K. VMD: visual molecular dynamics. *J Mol Graph*. 1996;**14**(1):27-38. doi: 10.1016/ 0263-7855(96)00018-5.
20. MATLAB and Statistics Toolbox. R2015a ed: The MathWorks Inc, Natick, Massachusetts, United States; 2015.
21. Pettersen EF, Goddard TD, Huang CC, Couch GS, Greenblatt DM, Meng EC, *et al*. UCSF Chimera--a visualization system for exploratory research and analysis. *J Comput Chem*. 2004;**25**(13):1605-1612. doi: 10.1002/jcc.20084.
22. Kumari R, Kumar R, Open Source Drug Discovery C, Lynn A. g_mmpbsa--a GROMACS tool for high-throughput MM-PBSA calculations. *J Chem Inf Model*. 2014;**54**(7):1951-1962. doi: 10.1021/ci500020m.
23. Kabsch W, Sander C. Dictionary of protein secondary structure: pattern recognition of hydrogen-bonded and geometrical features. *Biopolymers*. 1983;**22**(12):2577-2637. doi: 10.1002/bip.360221211.
24. Tien MZ, Meyer AG, Sydykova DK, Spielman SJ, Wilke CO. Maximum allowed solvent accessibilites of residues in proteins. *PLoS One*. 2013;**8**(11):e80635. doi: 10.1371/journal.pone.0080635.
25. Miller S, Janin J, Lesk AM, Chothia C. Interior and surface of monomeric proteins. *J Mol Biol*. 1987;**196**(3):641-656.doi: 10.1016/0022-2836(87)90038-6.
26. Wang Y, Schlamadinger DE, Kim JE, McCammon JA. Comparative molecular dynamics simulations of the antimicrobial peptide CM15 in model lipid bilayers. *Biochim Biophys Acta*. 2012;**1818**(5):1402-1409. doi: 10.1016/j.bbamem.2012.02.017.
27. Tashiro Y, Hasegawa Y, Shintani M, Takaki K, Ohkuma M, Kimbara K, *et al*. Interaction of Bacterial Membrane Vesicles with Specific Species and Their Potential for Delivery to Target Cells. *Front Microbiol*. 2017;**8**:571. doi: 10.3389/fmicb.2017.00571.
28. Li LB, Vorobyov I, Allen TW. The role of membrane thickness in charged protein-lipid interactions. *Biochim Biophys Acta*. 2012;**1818**(2):135-145.doi: 10.1016/j.bbamem.2011.10.026.
29. Bennett WF, Sapay N, Tieleman DP. Atomistic simulations of pore formation and closure in lipid bilayers. *Biophys J*. 2014;**106**(1):210-219. doi: 10.1016/j.bpj.2013.11.4486.
30. Kohut G, Sieradzan A, Zsila F, Juhasz T, Bosze S, Liwo A, *et al*. The molecular mechanism of structural changes in the antimicrobial peptide CM15 upon complex formation with drug molecule suramin: a computational analysis. *Phys Chem Chem Phys*. 2019;**21**(20):10644-10659. doi: 10.1039/c9cp00471h.
31. Andreu D, Ubach J, Boman A, Wahlin B, Wade D, Merrifield RB, *et al*. Shortened cecropin A-melittin hybrids. Significant size reduction retains potent antibiotic activity. *FEBS Lett*. 1992;**296**(2):190-194. doi: 10.1016/0014-5793(92)80377-s.
32. Wang G. Human antimicrobial peptides and proteins. *Pharmaceuticals (Basel)*. 2014;**7**(5):545-594.doi: 10.3390/ph7050545.
33. Domenech O, Sanz F, Montero MT, Hernandez-Borrell J. Thermodynamic and structural study of the main phospholipid components comprising the mitochondrial inner membrane. *Biochim Biophys Acta*. 2006;**1758**(2):213-221. doi: 10.1016/j.bbamem.2006.02.008.
34. Huang C, Li S. Calorimetric and molecular mechanics studies of the thermotropic phase behavior of membrane phospholipids. *Biochim Biophys Acta*. 1999;**1422**(3):273-307. doi: 10.1016/s0005-2736(99)00099-1.
35. McIntosh TJ, Simon SA. Area per molecule and distribution of water in fully hydrated dilauroylphosphatidylethanolamine bilayers. *Biochemistry*. 1986;**25**(17):4948-4952. doi: 10.1021/bi00365a034.
36. Thurmond RL, Dodd SW, Brown MF. Molecular areas of phospholipids as determined by 2H NMR spectroscopy. Comparison of phosphatidylethanolamines and phosphatidylcholines. *Biophys J*. 1991;**59**(1):108-113. doi: 10.1016/S0006-3495(91)82203-2.
37. Urbina JA, Moreno B, Arnold W, Taron CH, Orlean P, Oldfield E. A carbon-13 nuclear magnetic resonance spectroscopic study of inter-proton pair order parameters: a new approach to study order and dynamics in phospholipid membrane systems. *Biophys J*. 1998;**75**(3):1372-1383. doi: 10.1016/S0006-3495(98)74055-X.
38. Murzyn K, Rog T, Pasenkiewicz-Gierula M. Phosphatidylethanolamine-phosphatidylglycerol bilayer as a model of the inner bacterial membrane. *Biophys J*. 2005;**88**(2):1091-1103. doi: 10.1529/biophysj.104.048835.
39. Troskie AM, Rautenbach M, Delattin N, Vosloo JA, Dathe M, Cammue BP, *et al*. Synergistic activity of the tyrocidines, antimicrobial cyclodecapeptides from Bacillus aneurinolyticus, with amphotericin B and caspofungin against Candida albicans biofilms. *Antimicrob Agents Chemother*. 2014;**58**(7):3697-3707. doi: 10.1128/AAC.02381-14.
40. Schweppe DK, Harding C, Chavez JD, Wu X, Ramage E, Singh PK, *et al*. Host-Microbe Protein Interactions during Bacterial Infection. *Chem Biol*. 2015;**22**(11):1521-1530. doi: 10.1016/j.chembiol.2015.09.015.
41. Mangoni ML, Papo N, Barra D, Simmaco M, Bozzi A, Di Giulio A, *et al*. Effects of the antimicrobial peptide temporin L on cell morphology, membrane permeability and viability of *Escherichia coli*. *Biochem J*. 2004;**380**(Pt 3):859-865. doi: 10.1042/BJ20031975.
42. Brogden KA. Antimicrobial peptides: pore formers or metabolic inhibitors in bacteria? *Nat Rev Microbiol*. 2005;**3**(3):238-250. doi: 10.1038/nrmicro1098.
43. Huang HW, Chen FY, Lee MT. Molecular mechanism of Peptide-induced pores in membranes. *Phys Rev Lett*. 2004;**92**(19):198304. doi: 10.1103/PhysRevLett.92.198304.
44. Malanovic N, Lohner K. Antimicrobial Peptides Targeting Gram-Positive Bacteria. *Pharmaceuticals (Basel)*. 2016;**9**(3):59. doi: 10.3390/ph9030059.
45. Mishra NN, Bayer AS. Correlation of cell membrane lipid profiles with daptomycin resistance in methicillin-resistant Staphylococcus aureus. *Antimicrob Agents Chemother*. 2013;**57**(2):1082-1085. doi: 10.1128/AAC.02182-12.
46. Mileykovskaya E, Dowhan W. Cardiolipin membrane domains in prokaryotes and eukaryotes. *Biochim Biophys Acta*. 2009;**1788**(10):2084-2091. doi: 10.1016/j.bbamem.2009.04.003.
47. Feig M, MacKerell AD, Brooks CL. Force Field Influence on the Observation of π-Helical Protein Structures in Molecular Dynamics Simulations. *J Physical Chemistry B*. 2003;**107**(12):2831-2836. doi: 10.1021/jp027293y.